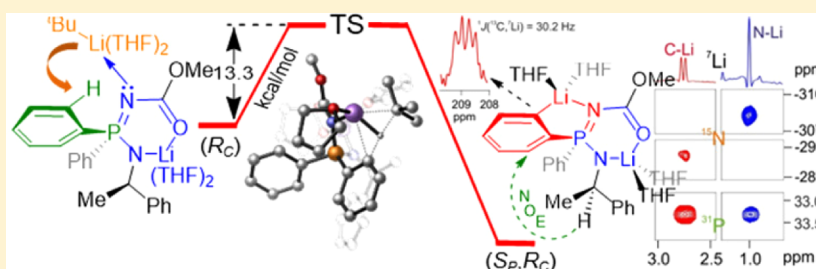


Diastereoselective Ortho Lithiation of Phosphinimidic Amides: A Multinuclear Magnetic Resonance and Computational Study

Fernando López Ortiz,* Jesús García López, María Casimiro, and María José Iglesias

Área de Química Orgánica, Universidad de Almería, Carretera de Sacramento s/n, 04120 Almería, Spain

S Supporting Information



ABSTRACT: The structure of the dianion (S_p,R_C)-**10** formed in the diastereoselective N,C_{ortho} dilithiation of the phosphinimidic amide (R_C)- $\text{Ph}_2\text{P}(=\text{NCO}_2\text{Me})\text{NHCH}(\text{Me})\text{Ph}$ (**5**; dr of 95:5) with *tert*-butyllithium in THF has been elucidated using multinuclear magnetic resonance methods, including 2D $^7\text{Li},^{15}\text{N}$ -HMQC ($^{15}\text{N}, ^{31}\text{P}$) correlations. (S_p,R_C)-**10** consists of a monomer in which C,N and N,O chelation of the lithium cations generates a system containing a five- and a six-membered metallacycle, respectively, sharing a P–N bond with the lithium atoms connected through the NCO moiety of the phosphazene group. Selective deprotonation of the *pro-S* P-phenyl ring of **5** was ascertained through NOE measurements. DFT computations at the M06-2X(SMD,THF)/6-311+G(d,p)//M06-2X/6-31G(d) level showed that the stereoselective ortho deprotonation process fulfills the features of the CIPE model. The P=N linkage of the N-lithiated species (R_C)-**8** acts as a directing metalation group via $\text{N}\cdots\text{Li}^t\text{Bu}$ coordination. The mixed complex that is formed evolves to a more stabilized species due to the intramolecular coordination of the OMe group to the lithium cation of the base. Abstraction of the ortho proton proceeds with energy barriers of 12.4 and 13.3 kcal/mol for the *pro-R* and *pro-S* phenyl rings. The preference for the latter is explained in terms of the Curtin–Hammett principle.

INTRODUCTION

The design and synthesis of P-stereogenic compounds are topics of great interest due to their applications in fields such as medicinal chemistry,¹ agrochemistry,² and particularly asymmetric synthesis in organic chemistry, where they play a critical role as organocatalysts³ or as ligands for transition-metal catalysis.⁴ One of the most useful methods of synthesis of this compound class is the enantioselective desymmetrization of Me_2P groups of phosphine–boranes via deprotonation with a chiral base, generally the complex $[\text{s-BuLi}\cdots(-)\text{-sparteine}]$,⁵ and subsequent electrophilic quench.⁶ In a similar vein, we have achieved the discrimination of the prochiral P-phenyl rings of the Ph_2P moiety of diphenylphosphinic amides and diphenylphosphinimidic amides through asymmetric directed ortho lithiation, DoLi, followed by electrophilic trapping of the ortho anion formed. The enantioselective abstraction of an ortho proton from *N,N*-diisopropyl-*P,P*-diphenylphosphinic amide **1** with the complex $[\text{s-BuLi}\cdots(-)\text{-sparteine}]$ as a chiral base followed by reaction with electrophiles afforded the derivatives (S_p)-**2** with modest ee (60%) (Scheme 1, eq 1). Access to enantiopure compounds was feasible by performing three recrystallization cycles.⁷ The deprotonation of substrates (*S*)-**3**⁸ and (*R*)-**5**⁹ bearing chiral amino moieties as chiral auxiliaries proved to be much more efficient. Both compounds underwent

N,C_{ortho} deprotonation with $t\text{BuLi}$ as a base with very high diastereoselectivity. After the dianions were treated with a large variety of electrophiles, the corresponding ortho-functionalized phosphinic amides (S_p,S_C)-**4** (Scheme 1, eq 2) and phosphinimidic amides (S_p,R_C)-**6** (Scheme 1, eq 3), respectively, were obtained in very high yield and an average dr of 95:5. Products **4** and **6** could be readily converted into other valuable P-stereogenic compounds such as phosphine–borane **7** through stereoselective functional group transformations.^{8,9} Recently, the first examples of transition-metal-assisted direct ortho C–H stereoselective functionalization of diphenylphosphinic amides have been described, although the structural diversity achieved is relatively limited.¹⁰

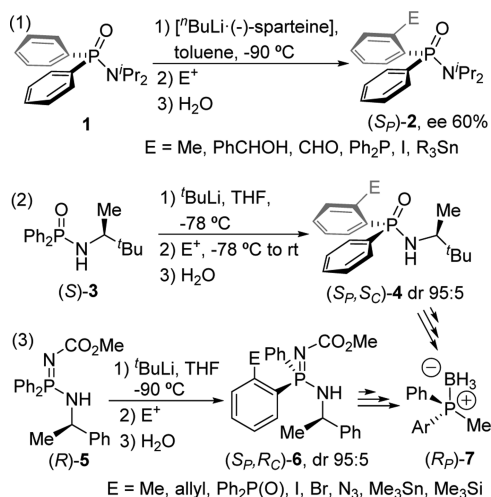
The first step in the ortho lithiation of **3** and **5** is the deprotonation of the NH of the amine moiety. The structure of the monoanion generated will determine the stereochemical course of the proton abstraction at the ortho position of one of the diastereotopic P-phenyl rings. Thus, whereas the N,C_{ortho} double lithiation of **3** takes place with excellent dr, the analogous reaction of the diphenylphosphinic amide having a 1-phenylethan-1-amine chiral auxiliary furnished the ortho-

Received: August 24, 2016

Published: October 7, 2016



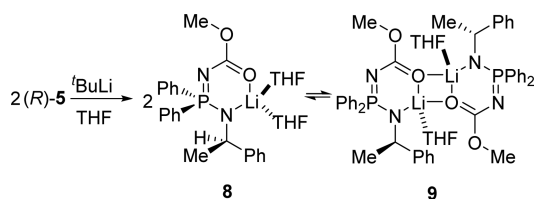
Scheme 1. Synthesis of P-Stereogenic Compounds through Asymmetric DoLi-Electrophilic Trapping Reactions



substituted products with very low stereocontrol (dr 1:2).¹¹ N-lithiated phosphinimidic amides are important ligands in coordination chemistry and catalysis.¹² Generally, the [N–P–N][−] system acts as a chelating monoanionic ligand that provides four-membered metallacycles upon binding to metal ions of the main groups and d and f blocks.¹³

Very recently, we have described the first detailed structural characterization of the N_α-lithiated phosphinimidic amide formed in the deprotonation of (R_C)-5 with 1 equiv of ^tBuLi in THF solution through nuclear magnetic resonance and DFT computational studies.¹⁴ The structure was shown to consist of a mixture of disolvated monomer 8 and monosolvated dimers 9 in which the anion exists as a six-membered metallacycle formed by coordination of the lithium ion to the deprotonated nitrogen and to the oxygen atom of the carbonyl group located in the phosphazene moiety (Scheme 2).¹⁵ The study revealed

Scheme 2. Formation of Monomers 8 and Dimers 9 in the N-Lithiation of (R)-5 in THF Solution



that the chiral side arm of the N,O-chelating framework is oriented to the outer face of the *pro-S* P-phenyl ring. Strictly speaking, these results indicate that the chiral auxiliary in 8 is close to only one of the P-phenyl rings and that the P=N linkage is in the appropriate arrangement to behave as a directing metalation group (DMG) in a DoLi process. This means that N-lithiation of (R_C)-5 leads to the system 8/9 preorganized for the stereoselective C_{ortho} lithiation. However, the reasons for the almost exclusive abstraction of one ortho proton of the *pro-S* P-phenyl ring of 8/9 by the action of a second equivalent of the organolithium base remain unclear. Under the premises of the CIPE model (complex induced proximity effect),¹⁶ the diastereoselectivity of the ortho deprotonation may be associated with the structure of the

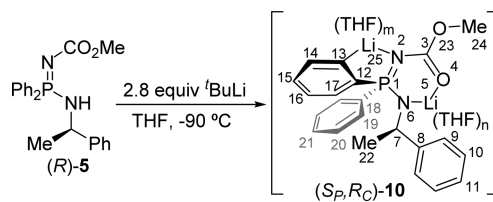
complex formed between the monolithiated species and the ^tBuLi.

In order to understand the reaction pathway of the highly diastereoselective N,C_{ortho} double deprotonation of (R)-5, we have undertaken a study of the structural characterization of the dilithiated species in THF solution on the basis of a series of multinuclear magnetic resonance experiments involving combinations of the nuclei ¹H, ⁷Li, ¹³C, ¹⁵N, and ³¹P and a DFT computational investigation of the mechanism of formation of the dianion within the framework of the CIPE model. We present herein the findings of this study.

RESULTS AND DISCUSSION

NMR Spectroscopic Studies. The synthesis of the N,C_{ortho} dilithiated species (S_p,R_C)-10 was carried out as previously described (Scheme 3).⁹ The treatment of (R_C)-5 with 2.8 equiv

Scheme 3. Synthesis of (S_p,R_C)-10 via N,C_{ortho} Double Lithiation of (R)-5



of ^tBuLi in THF (or THF-*d*₈) at −90 °C overnight afforded an orange solution. The configuration of 10 shown in Scheme 3 is assigned on the basis of the structure of the product of electrophilic quench (S_p,R_C)-6. All other structural features of the dianion were not known at the onset of this study. NMR samples were prepared by transferring 0.5 mL of this solution to a 5 mm NMR tube placed in a bath at −100 °C under an N₂ atmosphere. Subsequently, the samples were inserted into the magnet previously cooled to −80 °C.

The ⁷Li and ³¹P NMR spectra measured at this temperature showed that dilithiation of 5 was almost complete. The high diastereoselectivity observed for this reaction⁹ is in agreement with the presence of two different phosphorus signals at δ 33.35 and 28.46 ppm in the ratio 95:5 (Figure 1). Consequently, the

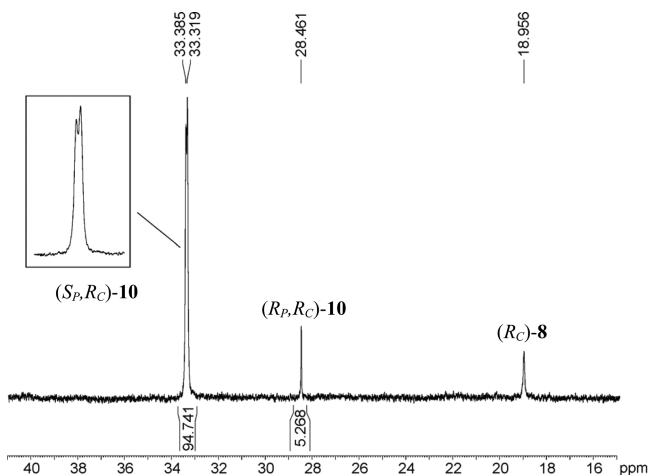


Figure 1. ³¹P NMR spectrum (202.4 MHz) of 10 measured in THF-*d*₈ at −80 °C. Exponential multiplication of the FID (LB = 1) prior to Fourier transformation.

major species was assigned to the dilithiated intermediate and the second species to the minor diastereoisomer (R_p, R_C)-**10**. The $^1\text{H}, ^{31}\text{P}$ -HMQC NMR experiment showed similar correlation patterns for the aromatic protons of both phosphorus signals (Figure S1 in the Supporting Information), confirming the formation of both diastereoisomers with excellent stereoselectivity. A very small amount (ca. 4%) of a third species was also detected and identified as the previously reported product of N-deprotonation (R_C)-**8**.¹⁴ The apparent doublet shape shown by the phosphorus signal of the dianion indicates the existence of a scalar coupling between the ^{31}P nuclei and the quadrupolar nucleus ^7Li ($I = 3/2$, 92.7% natural abundance). The unusual ^{31}P line shapes observed depend on relaxation effects¹⁷ and the magnitude of the scalar coupling.¹⁸ The lack of a resolved $^2J(^{31}\text{P}, ^7\text{Li})$ coupling constant prevents identification of the aggregation state of **10**.¹⁹

$N_{\omega}C_{\text{ortho}}$ dilithiation was evidenced in the ^1H NMR spectrum at $-100\text{ }^\circ\text{C}$ by (1) the disappearance of the NH signal which is associated with the reduction of the multiplicity of the adjacent proton H7 to a doublet of quartets (δ 4.51 ppm, $^3J_{\text{PH}} = 15.5$, $^3J_{\text{HH}} = 6.5$ Hz) (Figure S2 in the Supporting Information) and (2) the four multiplets arising from the ortho-deprotonated phenyl ring (δ 7.98 (H14), 6.67 (H15), 6.55 (H16), 7.12 (H17) ppm), which could be readily identified through the analysis of the 2D COSY45 NMR spectrum (Figure 2 and Figure S3 in the Supporting

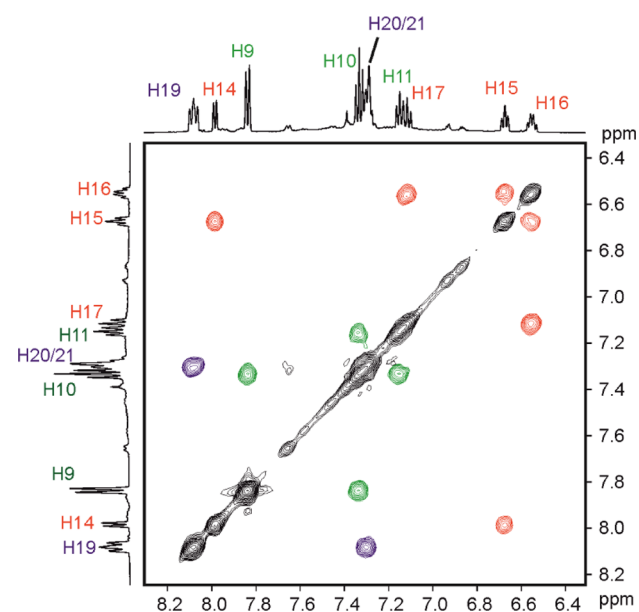


Figure 2. Expansion of the 2D COSY45 NMR spectrum (500.13 MHz) of **10** measured in THF- d_8 at $-80\text{ }^\circ\text{C}$. The three spin systems arising from the aromatic protons are identified by a color code.

Information). The assignment of the ortho proton H17 was easily accomplished by comparison of the ^1H and $^1\text{H}\{^{31}\text{P}\}$ NMR spectra on the basis of the large value of $^3J_{\text{PH}} = 8.2$ Hz observed for the signal at δ 7.12 ppm. The confirmation of the spin system defined by H14–H17 was provided by the 1D TOCSY spectrum obtained by selective excitation of the multiplet at δ 6.55 ppm, H16 (Figure S4 in the Supporting Information). The analogous experiment exciting selectively H7 allowed us to identify the methyl protons H22 (d, 1.33 ppm, $^3J_{\text{HH}} = 6$ Hz) that were masked by the solvent signals (pentane from the organolithium base) in the standard ^1H NMR

spectrum. The significant shielding experienced by H15–H17 in comparison with the chemical shifts observed for the protons of the nonsubstituted ring in the monolithiated intermediate **8** ($\Delta\delta_{10-8} \approx -0.6$ ppm) is remarkable. In sharp contrast, the proton next to the lithiated position H14 undergoes a significant deshielding ($\Delta\delta_{10-8} \approx 0.7$ ppm).²⁰

Analogous behavior was observed for their corresponding carbons in the ^{13}C NMR spectrum; C15, C16, and C17 appeared considerably shielded ($\Delta\delta_{10-8} \approx -5.3$, -6.8 , and -3.9 ppm, respectively),²⁰ whereas C14 is highly deshielded ($\Delta\delta_{10-8} \approx +14.4$ ppm).²⁰ In addition, there is a very large increase of the magnitude of the $^{31}\text{P}, ^{13}\text{C}$ coupling constants of C12 ($\Delta^1J_{\text{PC10-8}} \approx 17.5$ Hz), C14 ($\Delta^3J_{\text{PC10-8}} \approx 14.4$ Hz), and C17 ($\Delta^2J_{\text{PC10-8}} \approx 18$ Hz) (Figure 3 and Figures S5 and S6 in the

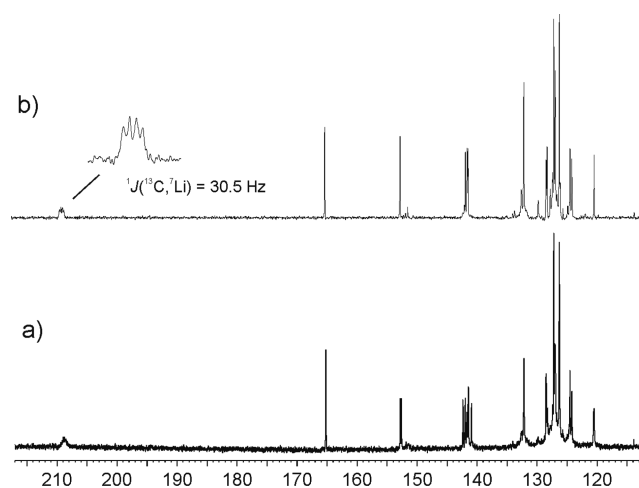


Figure 3. Expansion of the aromatic region of (a) ^{13}C and (b) $^{13}\text{C}\{^{31}\text{P}, ^1\text{H}\}$ NMR spectra (125.7 MHz) of **10** in THF- d_8 at $-100\text{ }^\circ\text{C}$. Gaussian multiplication of the FID (LB = -3 ; GB = 0.01) prior to Fourier transformation.

Supporting Information).²¹ These changes in the NMR parameters of the lithiated P-phenyl ring are similar to those found in ortho-lithium phosphinic amides²² and $C_{\omega}C_{\text{ortho}}$ dilithium phosphazenes.²³ The definitive evidence of the ortho-lithiation process was shown by the $^{13}\text{C}\{^{31}\text{P}, ^1\text{H}\}$ NMR spectrum, which exhibited a 1:1:1:1 quartet ($^2J_{\text{CLi}} = 30.2$ Hz) at δ 208.9 ppm assigned to the lithiated carbon C13.²⁴ The chemical shift²⁵ and the splitting of the signal of C13 reveal that it is in contact with only one ^7Li nucleus.¹⁹ For compounds where a lithium cation is bound to a carbon, the number of C–Li contacts can often be determined from the detection of the $^{13}\text{C}, ^7\text{Li}$ coupling constant. Except for ortho-lithiated phosphinic amides,²² ortho-lithium compounds tend to aggregate into dimers via C–Li–C bridges, leading to the formation of C_2Li_2 cores in the absence of strongly coordinating reagents.^{19c,26} The multiplicity observed for C13 indicates that dianion **10** exists as a monomer in THF solution. Most probably, the lithium atom is additionally coordinated to the nitrogen of the phosphazanyl moiety, thus forming a five-membered metallacycle, and would complete the preferred tetracoordination by solvation with two THF molecules.

The ^7Li NMR spectrum showed two predominant lithium signals in a 1:1 ratio, a doublet at δ 2.74 ppm (Li-A, $^2J_{\text{PLi}} = 8.0$ Hz) and a singlet at δ 0.99 ppm (Li-B), together with the corresponding signal of the N-lithiated species (R_C)-**8** (δ 0.95 ppm) (Figure 4). The assignment of the low-field signal to the

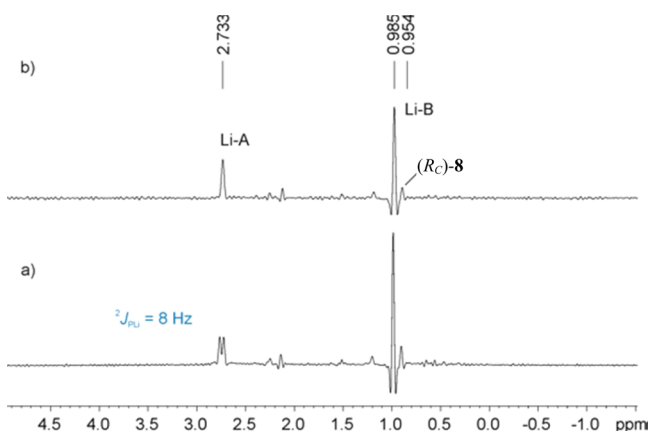


Figure 4. (a) ${}^7\text{Li}$ and (b) ${}^7\text{Li}\{{}^{31}\text{P}\}$ NMR spectra (194.4 MHz) of **10** measured in $\text{THF-}d_8$ at -80°C . Gaussian multiplication of the FID (LB = -20 ; GB = 0.1) prior to Fourier transformation.

lithium atom coordinated to the deprotonated nitrogen, Li–B, is supported by similarity to the chemical shift previously found for **8**.¹⁴ The high-field signal was assigned to a lithium atom linked to the C_{ortho} , Li–A. A 2D ${}^7\text{Li}$ -EXSY NMR experiment confirmed that the major species did not undergo chemical exchange with any other lithiated species present in the solution (Figure S8 in the Supporting Information).

As has been mentioned above, ortho-lithiated phosphinic amides tend to aggregate into dimers via O–Li–O bridges involving the P=O linkage.²² The multiplicity of the lithium is then affected by this coordination due to coupling with the two phosphorus atoms. With regard to our system, the multiplicity observed for Li–A implies that species **10** exists as a monomer in THF solution, as the lithium is coupled to only one phosphorus atom. The large magnitude of the coupling constant indicates the presence of P=N–Li coordination, which is in agreement with the formation of a five-membered metallacycle. Further confirmation was provided by a natural-abundance 2D ${}^7\text{Li}$, ${}^{15}\text{N}$ -HMQC NMR experiment (Figure 5). Two different correlations highlight the connection between the two lithium ions with the two different nitrogen atoms. Li–A is scalarly coupled to N2 (δ -288.7 ppm) and Li–B to N6 (δ -308.3 ppm). The ${}^{15}\text{N}$ chemical shifts are consistent with those recently described for intermediate **8** and previous data reported in the literature for similar phosphazenes.²⁷ As was expected, the 2D ${}^7\text{Li}$, ${}^{31}\text{P}$ -HMQC NMR experiment²⁸ showed correlation of both lithiums with the phosphorus. All this information revealed that the dilithiated intermediate **10** consists of a N, C_{ortho} and O, N_α double chelate, in which the phosphazenylium nitrogen stabilizes the ortho-lithiated position whereas the carboxymethyl fragment does the same with the lithium amide.

A 2D ROESY NMR experiment helped to elucidate the conformation adopted by species **10** in solution (Figure 6 and Figure S9 in the Supporting Information). The spectrum showed two NOEs for the ortho proton of the metalated ring H17, one with the methine proton of the chiral auxiliary H7 and the other with H19 (δ 8.08 ppm, ${}^3J_{\text{HH}} = 6.7$ Hz, ${}^3J_{\text{PH}} = 8.2$ Hz), belonging to the neighboring P-phenyl ring. On the other hand, H19 exhibits a dipolar correlation with H9, the phenyl ring of the chiral auxiliary. These complementary NOEs support that the structure of the dilithiated intermediate **10** in solution consists of a configurationally stable N,O/N,C double chelate, in which the relative configuration at the phosphorus is

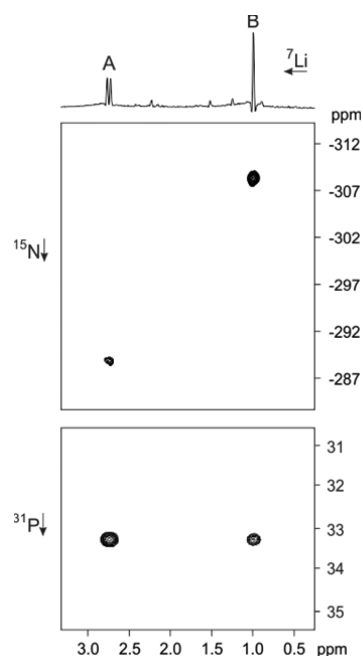


Figure 5. ${}^7\text{Li}$, ${}^{15}\text{N}$ -HMQC and ${}^7\text{Li}$, ${}^{31}\text{P}$ -HMQC correlation spectra of **10** in $\text{THF-}d_8$ measured at -100°C .

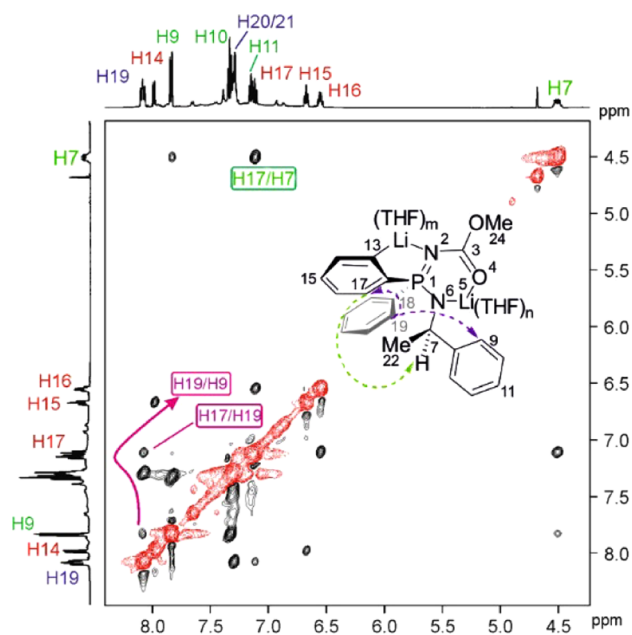


Figure 6. Expansion of the 2D ROESY NMR spectrum of **10** measured in $\text{THF-}d_8$ at -80°C .

S. The lack of interaction between the methoxy group and any other protons of the dianion is consistent with the coordination between the carbonyl group and Li–A, which allocates this group in an isolated position with regard to the rest of the molecule.

As has been mentioned above, the conformation adopted by the monolithiated intermediate **8** in solution is responsible for directing the ortho lithiation with excellent diastereoselectivity. Species **8** was shown to exist in THF as a monomer–dimer equilibrium mixture shifted to the monomeric species in highly diluted samples, which represent the standard laboratory-scale reaction conditions (0.05 M). With regard to dianion **10**, the

Table 1. Selected Distances (Å) and Angles (deg) of **8a,c**, **11A,B**, and **12A,B**^a

param	8a	8c	11A	11B	12A	12B
P1–N2	1.643	1.641	1.664	1.657	1.654	1.638
P1–N6	1.601	1.612	1.597	1.608	1.598	1.597
N2–C3	1.328	1.322	1.331	1.328	1.328	1.323
C3–O4	1.254	1.259	1.251	1.249	1.246	1.242
O4–Li5	1.875	1.890	1.898	1.894	1.940	1.907
N2–Li25			2.146	2.160	2.047	2.018
Li5–N6	1.977	1.963	1.963	1.977	1.962	1.965
O23–Li25			2.825	2.952	2.445	2.200
P1–N6–Li5	106.1	106.4	109.3	111.5	109.3	109.9
P1–N6–C7	125.2	122.3	125.3	118.4	123.6	119.7
C7–N6–Li5	128.6	126.2	125.3	125.4	126.9	127.1
C3–N2–P1–N6	51.0	–49.6	51.8	37.3	48.4	–31.7
C3–O4–Li5–N6	26.0	–39.6	44.5	19.6	32.2	–41.3
P1–N6–Li5–O4	16.5	0.5	4.2	20.8	10.3	26.8
P1–N2–C3–O4	0.0	3.6	4.3	9.7	2.4	18.2
P1–N6–C7–C8	103.3	58.4	124.2	137.6	88.3	133.9
P1–N6–C7–C22	–134.3	–180.3	–112.4	–100.3	–148.3	–104.0

^aThe numbering scheme is referenced to (*S_pR_C*)-**10**; see Scheme 3.

multiplicity observed for the lithiated carbon C13 and the lithium nucleus Li-A were critical parameters toward drawing the definitive structure for the lithiated intermediate as a monomeric species. However, the possible formation of dimers through O–Li bridges such as **9** (Scheme 2) and *C_α*-lithiated *N*-methoxycarbonylphosphazenes **5**¹⁵ could only be discarded by studying the concentration dependence. No significant changes were observed in the ³¹P NMR spectrum of diluted samples of **10**, confirming the existence of the dilithiated species as a monomer in THF solution. As far as we know, this is the first structural characterization of an enantiopure dilithiated phosphinimidic amide.

Computational Studies. Once the structure of the NC_{ortho} dilithiated species (*S_pR_C*)-**10** was identified, we undertook a DFT computational study at the M06-2X(SMD,THF)/6-311+G(d,p)//M06-2X/6-31G(d) level of theory to get insight into the mechanism of its formation via diastereoselective ortho deprotonation of the *pro-S* P-phenyl ring of (*R_C*)-**8**. For simplicity, the computations have been based on the structure of dissolvated monomer (*R_C*)-**8**.²⁹ Selected geometrical parameters for the computed species are given in Table 1. Previous calculations about the structure of (*R_C*)-**8** were carried out at the M06-2X(SMD,THF)/6-311+G(d,p)//B3LYP/6-31G(d) level of theory. They revealed that the six-membered metallacycle of (*R_C*)-**8** may adopt two twist-boat conformations and that for each of them the methoxy group may be oriented syn or anti with respect to the nitrogen atom of the NCO₂Me moiety.¹⁴ First, we have optimized the geometries of these four conformers at the higher level of calculation used in this work. The two conformers involved in the ortho lithiation, (*R_C*)-**8a** and (*R_C*)-**8b**, exist in a slightly twisted boat conformation (P1–N2–C3–O4/P1–N6–Li5–O4 angles of 0.0/16.5° and –1.2/14.1° for **8a** and **8b**, respectively, Table 1). In both cases, the pseudoequatorial P-phenyl ring is eclipsed with the CH of the chiral arm³⁰ and, perhaps most importantly, the pseudoaxial P-phenyl is oriented quasi-perpendicular to the phenyl linked to the chiral center (Figure S10 in the Supporting Information). The almost linear alignment of one ortho C–H bond of the P-phenyl ring with the centroid of the C-phenyl group (C–H-centroid angles of 174.9 and 174.7° for **8a** and **8b**, respectively) and the short CH⋯centroid distances (2.790 and 2.805 Å for

8a and **8b**, respectively) are in the expected range for a T-shaped edge-to-face C–H⋯π interaction.³¹ Conformers **8a** and **8b** differ in the relative position of the OMe group with respect to the adjacent nitrogen atom, with the syn orientation of structure **8a** (N2–C3–O23–C24 angle of –1.5°) being negligibly stabilized in comparison with the anti rotamer **8b** (Δ*G*¹⁸³(**8a**–**8b**) = 0.2 kcal/mol, N2–C3–O23–C24 angle of –178.1°).³² It is important to note that structures **8a** and **8b** are not the most stable N-lithiated species. At the level of calculation used, the isomer **8c** in which the twisted conformation of the six-membered ring is inverted with respect to **8a** proved to be 0.4 kcal/mol more stable (Figure S10). In the same vein, the isomer **8d** with the conformation of the metallacycle mirroring that of **8b** is stabilized 0.3 kcal/mol in comparison with **8a**. The energy differences between the pairs of conformers **8a/8b** and **8c/8d** of only 0.2 and 0.1 kcal/mol, respectively, indicate that the conformations of the metallacycle and the OMe group may interconvert very easily. Therefore, the reaction pathway for the abstraction of an ortho proton of **8** will be determined by the relative energies of some other intermediate species involved in the reaction coordinate. The calculations showed that the two most favorable deprotonations occurred for **8a** and **8b** (see below). In the following, we will focus on the ortho lithiation of these two species.

According to the CIPE model,¹⁶ the P=N moiety of monoanion **8** is in the appropriate arrangement to act as a DMG in a DoLi reaction.³³ The CIPE model establishes that a prelithiation complex is responsible for bringing the reactive groups into proximity for directed deprotonation. In this scenario, the formation of (*S_pR_C*)-**10** indicates that the phosphinimidic nitrogen of (*R_C*)-**8** would coordinate to the lithium cation of the ^tBuLi base and the resulting complex would show a conformation in which abstraction of the ortho proton of the *pro-S* phenyl ring becomes highly favored. ^tBuLi exists as a monomer in THF solution.³⁴ Furthermore, computational studies showed that the most stable structure consists of a trisolvated alkyllithium monomer.³⁵ Therefore, building up a mixed organolithium complex between (*R_C*)-**8** and ^tBuLi in THF will involve the desolvation of one THF molecule from the base. This process is thermodynamically favorable for both pathways involving the abstraction of one

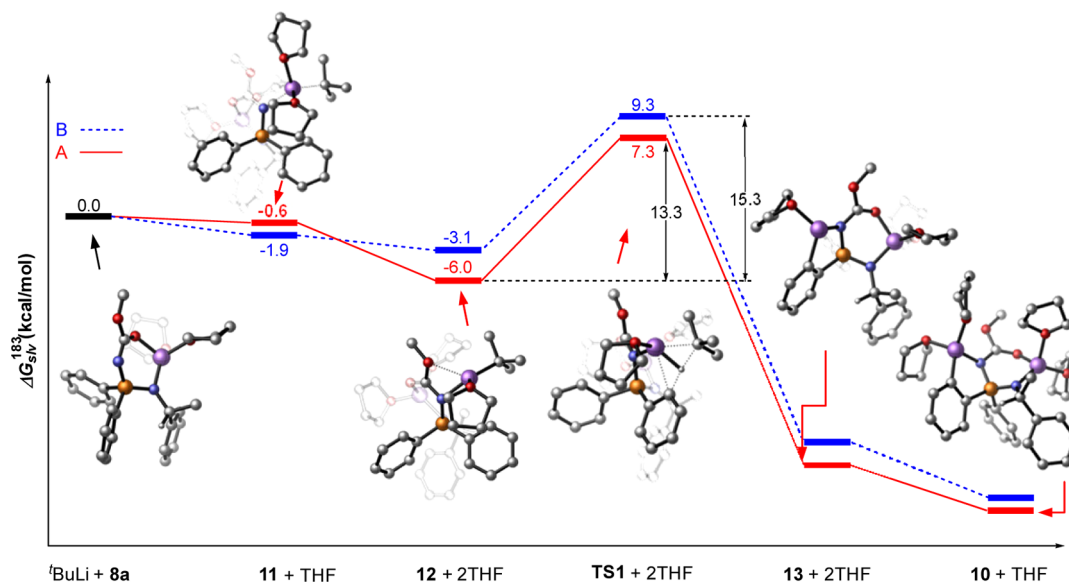


Figure 7. Computed pathways for the diastereoselective ortho deprotonation of (R_C) -8 with $t\text{BuLi}$. Hydrogen atoms have been omitted for clarity, except for the H_{ortho} being abstracted in TS1.

pro-S (pathway A) and one *pro-R* (pathway B) ortho proton from (R_C) -8b to give complexes 11A and 11B, respectively (Figure 7 and Figure S11 in the Supporting Information). The formation of 11B is slightly more exothermic by 1.3 kcal/mol. Interestingly, the analogous coordination of $t\text{BuLi}$ to the $\text{P}=\text{N}$ linkage of (R_C) -8a that would lead to the deprotonation of the *pro-S* phenyl ring via complex 11C (path C) is endothermic ($\Delta G^{183} = 3.4$ kcal/mol, Figure S12 in the Supporting Information). Since rotamer (R_C) -8b is destabilized only by 0.2 kcal/mol with respect to (R_C) -8a, it can be reasonably assumed that the DoLi reaction of *N*-lithiated 8 proceeds through the species (R_C) -8b.

The bond distances in the metallacycle are insensitive to the $t\text{BuLi}$ complexation (Table 1) except for a slight increase in the $\text{P}=\text{N}$ bond length of 11A/11B (1.664/1.657 Å) in comparison with 8a (1.664/1.657 Å). The conformation in 11A is similar to that of 8a, whereas it becomes more puckered in 11B (Table 1). The structure of 11B shows that the approach of the organolithium base to the *pro-R* phenyl ring of 8a induces a rotation of the chiral side arm that allocates the C–H almost on the bisection of the $\text{Ph}-\text{P}-\text{Ph}$ angle and the methyl group facing the pseudoequatorial *pro-S* P-phenyl ring ($\text{P1}-\text{N6}-\text{C7}-\text{C23}$ torsion angle of $-112.4/-100.3^\circ$ for 11A/11B, Table 1). In complexes 11A/11B the carbanionic center of the $t\text{Bu}$ moiety is located close to a *pro-S/pro-R* ortho proton showing $\text{C}\cdots\text{H}_{\text{ortho}}$ distances of 2.456/2.449 Å, notably shorter than the sum of the respective van der Waals (vdW) radii (2.900 Å). Important sub van der Waals distances have also been found between the oxygen atom of the methoxy group and the lithium of $t\text{BuLi}$ ($\text{O}\cdots\text{Li}$ distances of 2.825/2.952 Å for 11A/11B; sum of vdW radii of 3.340 Å).

The $\text{MeO}\cdots\text{Li}$ proximity is responsible for the transformation that complexes 11A and 11B undergo prior to ortho proton abstraction. This weak interaction progresses along the reaction coordinate to become an $\text{O}-\text{Li}$ bond (2.445/2.201 Å for 12A/12B) with simultaneous displacement of a THF molecule from the coordination sphere of lithium leading to two new complexes 12A and 12B (Figure 7 and Figure S13 in the Supporting Information).³⁶ Although the $\text{O23}-\text{Li25}$ interaction is stronger in 12B (bond distance of 2.200 Å) than in

12A (bond distance of 2.445 Å), the formation of the latter complex is notably more exothermic ($\Delta G^{183} = -6.0$ kcal/mol for 12A and -3.1 kcal/mol for 12B with respect to (R_C) -8a). This higher stabilization can be at least in part assigned to the existence of a $\text{C}-\text{H}\cdots\pi$ interaction between one ortho proton of the pseudoaxial P-phenyl ring and the phenyl of the chiral moiety ($\text{C}-\text{H}\cdots\text{centroid}$ distance of 2.507 Å).³¹

Complexes 12A and 12B are converted via the transition states TS1A and TS1B into the respective ortho-deprotonated species (S_P, R_C) -13A and (R_P, R_C) -13B (Figure 8 and Figures S14 and S15 in the Supporting Information). The process is highly exothermic in both cases, leading to products of similar stability ($\Delta G^{183}(13A) = -17.1$ kcal/mol and $\Delta G^{183}(13B) = -17.8$ kcal/mol). The energy of activation for the abstraction of

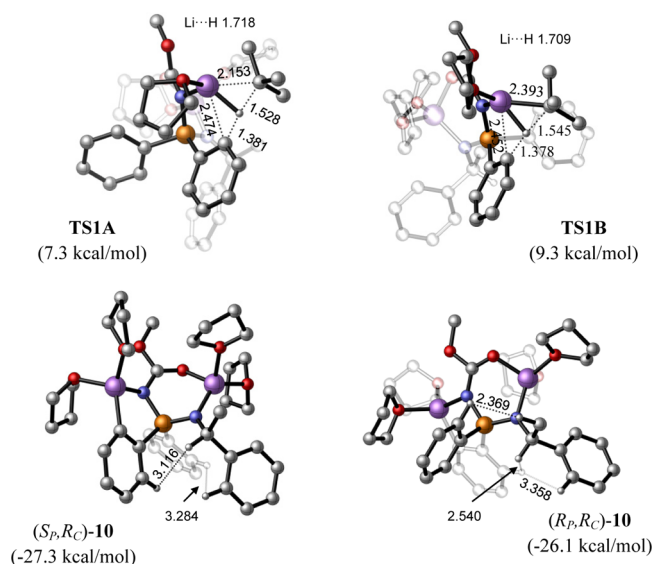


Figure 8. Computed structures of the most stable transition states TS1A and TS1B corresponding to the ortho deprotonation of the *pro-S* and *pro-R* phenyl ring, respectively, and diastereomeric end N,C_{ortho} dianions 10.

the *pro-R* proton is slightly lower ($\Delta G^{\ddagger 183} = 12.4$ kcal/mol) than for the *pro-S* proton ($\Delta G^{\ddagger 183} = 13.3$ kcal/mol). These results seem to suggest that, contrary to the experimental observations, the formation of the stereoisomer of R_p,R_C configuration would be favored by $\Delta\Delta G^{\ddagger 183} = -0.9$ kcal/mol. However, if we assume that complexes **8a** and **8b** interconvert rapidly ($\Delta\Delta G^{\ddagger 183} = 0.2$ kcal/mol), then according to the Curtin-Hammett principle the outcome of the reaction will be controlled by the activation energies calculated with respect to the most stabilized complex **12A**. The lower energy barrier for the formation of (S_p,R_C) -**13A** vs (R_p,R_C) -**13B** by 2 kcal/mol is in agreement with the reported almost exclusive lithiation of the *pro-S* phenyl ring.³⁷

The six-membered ring of **TS1A** adopts a slightly distorted half-chair conformation (angles O4–C3–N2–P1 -2.7° , O4–Li5–N6–P1 11.4°), whereas the metallacycle of **TS1B** exists in a twist-boat configuration (angles O4–C3–N2–P1 13.1° , O4–Li5–N6–P1 28.4°). The geometries of the transition states show that the removal of the ortho proton is more advanced in **TS1A** than in **TS1B**. The distance between the quaternary carbon of the ^tBu group and the H13 proton being abstracted in **TS1A** (1.528 Å) is shorter than in **TS1B** (1.545 Å). Conversely, all other distances involving H13 and Li25 in **TS1A** lengthen with respect to **TS1B** (Figure 8). The largest difference proceeds from the methoxy group and the adjacent lithium atom. The distances O23...Li25 of 3.016/2.705 Å in **TS1A/TS1B** indicate a loose/tight coordination, respectively.

Expectedly, dianions **13A** and **13B** undergo additional stabilization when the lithium cation Li25 is allowed to coordinate to a second THF molecule to achieve the usually most favorable tetracoordination state of a lithium cation.^{18,19} The computed $N_{ortho}C_{ortho}$ dilithiated final products (S_p,R_C) -**10a** ($\Delta G^{183} = -27.3$ kcal/mol) and (R_p,R_C) -**10b** ($\Delta G^{183} = -26.1$ kcal/mol) are rigid tricyclic systems built by bridging the two lithium atoms through the heteroatoms of the NCO moiety of the phosphazanyl group (Figures 7 and 8 and Figure S16 in the Supporting Information). Similarly to previous intermediate species, the six-membered metallacycle of **10a** exists in a twist-boat conformation (angles O4–C3–N2–P1 -178.1° , O4–Li5–N6–P1 6.0°) containing two planar nitrogen atoms. As for the chiral side arm, the C–H is eclipsed with the P–C bond of the ortho-lithiated ring and the phenyl group is located almost perpendicular to the unsubstituted P-phenyl ring at a distance favorable to the existence of a $PC_{Ar}-H_{ortho}\cdots\pi$ interaction (distance to the centroid of 2.792 Å, C–H...centroid angle of 174.0°).³⁸ In this arrangement, H9 is close to H17 and H19, while H7 is found only in the vicinity of H9 (distances in the range of 2.817–3.440 Å), in excellent agreement with the NOEs detected in the ROESY spectrum of (S_p,R_C) -**10** measured at -80°C (Figure 6).

CONCLUSIONS

In summary, the structure of the enantiomerically pure $N_{ortho}C_{ortho}$ -dilithiated aminophosphazene (S_p,R_C) -**10** in THF solution has been elucidated. (S_p,R_C) -**10** was formed by treating aminophosphazene **5** with 2.8 equiv of ^tBuLi via the N-lithiated species **8** in a diastereomeric ratio of 95:5. A multinuclear magnetic resonance study including $^{13}\text{C}\{^3\text{P},^1\text{H}\}$ and $^7\text{Li}\{^1\text{H}\}$ HMQC (^1H , ^{13}C , ^3P) NMR triple-resonance experiments revealed that the dianion exists in THF solution at -80°C as a monomer in which the aminophosphazene moiety exhibits N,O and C,N double chelation to two lithium cations as part of six- and five-membered metallacycles, respectively. The NOEs

observed in the ROESY spectrum support the existence of a preferred conformation with the CH and the phenyl groups of the chiral side arm located close to the ortho-substituted and unsubstituted P-phenyl rings, respectively. The DFT computational investigation of the diastereoselective ortho deprotonation of (R_C) -**8** provided a reaction pathway in agreement with the CIPE model. Complexation of ^tBuLi·THF₃ by lithium coordination of the phosphazanyl nitrogen of (R_C) -**8** is slightly exothermic and is accompanied by the desolvation of a THF molecule. The resulting mixed complex undergoes additional stabilization through intramolecular coordination of the OMe group to the lithium cation of the ^tBuLi prior to proton abstraction to afford the $N_{ortho}C_{ortho}$ -dilithiated intermediate species **13**·THF₃, which evolves into the final product (S_p,R_C) -**10**·THF₄ by solvation of the lithium bound to the ortho carbon to a THF molecule to achieve tetracoordination. The very high diastereoselectivity of the ortho deprotonation is explained on the basis of the Curtin–Hammett principle: fast interconversion of the initial mixed complexes corresponding to the approach of the organolithium base to the *pro-R* and *pro-S* P-phenyl rings and a difference of 2 kcal/mol between the corresponding transition states.

EXPERIMENTAL SECTION

General Information. All reactions and manipulations were carried out under a dry N₂ gas atmosphere using standard Schlenk procedures. THF-*d*₈ was distilled from sodium/benzophenone immediately prior to use. ^tBuLi was purchased and used as received. Low temperatures were always achieved with a N₂(l)/MeOH bath. Multinuclear magnetic resonance spectra were measured in a 11.74 T spectrometer (¹H, 500.13 MHz; ⁷Li, 194.37 MHz; ¹³C, 125.76 MHz; ¹⁵N, 50.67 MHz; ³¹P, 202.46 MHz) using a direct TBO ¹H/³¹P/BB. The spectral references used were internal tetramethylsilane for ¹H and ¹³C, MeNO₂ for ¹⁵N, external 85% H₃PO₄ for ³¹P, and 1 M LiBr in D₂O for ⁷Li. A set of two complementary ³¹P/⁷Li-selective band-pass/stop frequency filters was used for the measurement of NMR spectra involving ³¹P and ⁷Li nuclei. Selected spectral parameters were as follows: ⁷Li NMR (194.4 MHz): 24K data points; spectral width 9690 Hz; exponential multiplication with a line broadening factor of 2 Hz. For resolution enhancement processing a Gaussian multiplication (GM) was applied to ⁷Li (LB = -2, GB = 0.3). ³¹P NMR (202.4 MHz): 128K data points; spectral width 60606 Hz; exponential multiplication with a line broadening factor of 2 Hz. The ⁷Li,³¹P{¹H} HMQC 2D experiment was performed using spectral widths of 5399 Hz (³¹P) and 2717 Hz (⁷Li), a final matrix after zero filling of 1024 × 128, and an evolution delay for $^nJ_{PL}$ of 50 ms. The ⁷Li,¹⁵N HMQC 2D experiment was performed using spectral widths of 20271 Hz (¹⁵N) and 2717 Hz (⁷Li), a final matrix after zero filling of 1024 × 256, and an evolution delay for $^nJ_{NL}$ of 50 ms. The ³¹P,¹⁵N{¹H} HMQC 2D experiment was performed using spectral widths of 20271 Hz (¹⁵N) and 5081 Hz (³¹P), a final matrix after zero filling of 1024 × 128, and an evolution delay for $^nJ_{PN}$ of 17 ms.

Computational Details. The geometries of all compounds were optimized with the meta-hybrid density functional M06-2X³⁹ and a 6-31G(d) basis set in the gas phase. Single-point energy calculations were performed with the M06-2X functional and a 6-311+G(d,p) basis. The performance of this functional proved to be superior to that of the B3LYP previously used for the computations of the N-lithiated species.¹⁴ The SMD⁴⁰ solvation model was used in M06-2X single-point energy calculations. THF was used as the solvent. All stationary points were characterized as minimum or transition states and checked by vibrational analysis. The reported free energies and enthalpies include zero-point energies and thermal corrections calculated at 183 K. Entropic contributions to the reported free energies were calculated from partition functions evaluated with the quasi-harmonic approximation of Truhlar and co-workers.⁴¹ All calculations were performed

with Gaussian 09.⁴² The 3D structures of molecules were generated using CYLView (<http://www.cylview.org>)

General Procedure for the Dilithiation of (R)-5 and NMR Sample Preparation. To a solution of phosphinimidic amide (R)-5 (0.4 mmol) in THF (5 mL) was added a solution of *t*-BuLi (0.7 mL of a 1.7 M solution in cyclohexane; 1.12 mmol; 2.8 equiv) at $-90\text{ }^{\circ}\text{C}$. After 15 h of metalation, 0.5 mL of the reaction mixture was transferred to a 5 mm NMR tube under an N_2 atmosphere placed in a refrigerated bath at $-100\text{ }^{\circ}\text{C}$. Subsequently, the sample was transferred to a magnet previously cooled to $-90\text{ }^{\circ}\text{C}$. A set of 1D and 2D NMR spectra were acquired in the temperature range of -110 to $-70\text{ }^{\circ}\text{C}$ to elucidate the structure of ($S_{\text{P}},R_{\text{C}}$)-10 (Figures S1–S9 in the Supporting Information). $\text{N}_2\text{C}_{\text{ortho}}$ -dilithium ($S_{\text{P}},R_{\text{C}}$)-10 (spectra measured at $-100\text{ }^{\circ}\text{C}$): ^1H NMR (THF- d_6 , 500.13 MHz) δ 1.33 (d, 3H, $^3J_{\text{HH}} = 6.5$ Hz, H22), 3.53 (s, 3H, H24), 4.51 (dc, 1H, $^3J_{\text{PH}} = 15.5$, $^3J_{\text{HH}} = 6.5$ Hz, H7), 6.55 (dt, 1H, $^3J_{\text{HH}} = 6.9$, $^4J_{\text{PH}} = 5.8$ Hz, H16), 6.67 (t, 1H, $^3J_{\text{HH}} = 6.9$ Hz, H15), 7.12 (dd, 1H, $^3J_{\text{PH}} = 8.2$, $^3J_{\text{HH}} = 6.9$ Hz, H17), 7.15 (t, 1H, $^3J_{\text{HH}} = 7.5$ Hz, H11), 7.29 (m, 3H, H20, H21), 7.32 (m, 2H, H10), 7.85 (d, 1H, $^3J_{\text{HH}} = 7.5$ Hz, H9), 7.98 (d, 1H, $^3J_{\text{HH}} = 6.9$ Hz, H14), 8.08 (m, 1H, H19) ppm; ^{13}C NMR (THF- d_6 , 125.76 MHz) δ 22.9 (d, C22), 50.8 (s, C24), 52.1 (s, C7), 120.5 (d, $^3J_{\text{PC}} = 15.5$ Hz, C16), 124.2 (s, C15), 124.5 (s, C11), 126.3 (s, C9), 127.0 (d, $^3J_{\text{PC}} = 15.5$ Hz, C20), 127.2 (s, C10), 128.3 (d, $^3J_{\text{PC}} = 26.4$ Hz, C17), 128.5 (s, C21), 132.2 (d, $^2J_{\text{PC}} = 7.0$ Hz, C19), 141.5 (d, $^1J_{\text{PC}} = 131.3$ Hz, C12), 141.6 (d, $^2J_{\text{PC}} = 26.2$ Hz, C14), 141.9 (d, $^1J_{\text{PC}} = 115.6$ Hz, C18), 152.7 (d, $^3J_{\text{PC}} = 23.3$ Hz, C8), 165.2 (s, C3), 208.9 (m, $^3J_{\text{C}=\text{Li}} = 30.5$ Hz, C13) ppm; ^{31}P NMR (THF- d_6 , 202.46 MHz) δ 33.3 ppm; ^7Li NMR (THF- d_6 , 194.37 MHz) δ 1.0 (s, Li5), 2.74 (d, $^2J_{\text{PLi}} = 8.0$ Hz, Li25) ppm; ^{15}N NMR (THF- d_6 , 50.67 MHz) δ -288.7 (N2), -308.3 (N5) ppm.

■ ASSOCIATED CONTENT

● Supporting Information

The Supporting Information is available free of charge on the ACS Publications website at DOI: 10.1021/acs.joc.6b02083.

1D and 2D NMR spectra of species 10, DFT computed structures for the formation of 10, reference for Gaussian 09, and Cartesian coordinates and energies of the stationary points located (PDF)

■ AUTHOR INFORMATION

Corresponding Author

*E-mail for F.L.O.: flortiz@ual.es.

Notes

The authors declare no competing financial interest.

■ ACKNOWLEDGMENTS

We thank the MINECO and FEDER program for financial support (projects CTQ2011-27705 and CTQ2014-57157-P). M.C. thanks the MICINN for a Ph.D. fellowship.

■ REFERENCES

- (a) Guga, P. *Curr. Top. Med. Chem.* **2007**, *7*, 695. (b) Virieux, D.; Volle, J.-N.; Bakalara, N.; Pirat, J.-L. *Top. Curr. Chem.* **2014**, *360*, 39. (c) Wiemer, A. J.; Wiemer, D. F. *Top. Curr. Chem.* **2014**, *360*, 115. (d) Pertusati, F.; McGuigan, C. *Chem. Commun.* **2015**, *51*, 8070.
- (2) Sasaki, M. *Phosphorus, Sulfur Silicon Relat. Elem.* **2008**, *183*, 291.
- (3) (a) Wei, Y.; Shi, M. *Acc. Chem. Res.* **2010**, *43*, 1005. (b) Rémond, E.; Bayardon, J.; Takizawa, S.; Rousselin, Y.; Sasai, H.; Jugé, S. *Org. Lett.* **2013**, *15*, 1870. (c) Warner, C. J. A.; Reeder, A. T.; Jones, S. *Tetrahedron: Asymmetry* **2016**, *27*, 136.
- (4) (a) Lühr, S.; Holz, J.; Börner, A. *ChemCatChem* **2011**, *3*, 1708. (b) *P-Chiral Ligands in Phosphorus(III) Ligands in Homogeneous Catalysis: Design and Synthesis*; Kamer, P. C. J., van Leeuwen, P. W. N. M., Eds.; Wiley: Chichester, U.K., 2012. (c) Standley, E. A.; Tasker, S. Z.; Jensen, K. L.; Jamison, T. F. *Acc. Chem. Res.* **2015**, *48*, 1503. For

recent references see: (d) Xu, Y.; Yang, Z.; Ding, B.; Liu, D.; Liu, Y.; Sugiya, M.; Imamoto, T.; Zhang, W. *Tetrahedron* **2015**, *71*, 6832. (e) Orgue, S.; Flores-Gaspar, A.; Biosca, M.; Pamies, O.; Dieguez, M.; Riera, A.; Verdager, X. *Chem. Commun.* **2015**, *51*, 17548. (f) Hu, Q.; Chen, J.; Zhang, Z.; Liu, Y.; Zhang, W. *Org. Lett.* **2016**, *18*, 1290. (g) Schmitz, C.; Holthusen, K.; Leitner, W.; Francio, G. *ACS Catal.* **2016**, *6*, 1584. (h) Dutartre, M.; Bayardon, J.; Jugé, S. *Chem. Soc. Rev.* **2016**, *45*, 5771.

(5) Muci, A. R.; Campos, K. R.; Evans, D. A. *J. Am. Chem. Soc.* **1995**, *117*, 9075.

(6) (a) O'Brien, P. *Chem. Commun.* **2008**, 655–667. (b) Harvey, J. S.; Gouverneur, V. *Chem. Commun.* **2010**, *46*, 7477. (c) Kolodiazhnyi, O. I. *Top. Curr. Chem.* **2014**, *360*, 161. (d) Alayrac, C.; Lakhdar, S.; Abdellah, I.; Gaumont, A.-C. *Top. Curr. Chem.* **2014**, *361*, 1.

(7) Popovici, C.; Oña-Burgos, P.; Fernández, I.; Rocas, L.; García-Granda, S.; Iglesias, M. J.; López-Ortiz, F. *Org. Lett.* **2010**, *12*, 428.

(8) del Águila-Sánchez, M. A.; Navarro, Y.; López, J. G.; Guedes, G. P.; López-Ortiz, F. *Dalton Trans.* **2016**, *45*, 2008.

(9) Casimiro, M.; Guedes, G. P.; Iglesias, M. J.; López-Ortiz, F. *Tetrahedron: Asymmetry* **2015**, *26*, 53 and references therein.

(10) (a) Gwon, D.; Lee, D.; Kim, J.; Park, S.; Chang, S. *Chem. - Eur. J.* **2014**, *20*, 12421. (b) Du, Z.-J.; Guan, J.; Wu, G.-J.; Xu, P.; Gao, L.-X.; Han, F.-S. *J. Am. Chem. Soc.* **2015**, *137*, 632. (c) Liu, L.; Zhang, A.-A.; Wang, Y.; Zhang, F.; Zuo, Z.; Zhao, W.-X.; Feng, C.-L.; Ma, W. *Org. Lett.* **2015**, *17*, 2046. (d) Lin, Z.-Q.; Wang, W.-Z.; Yan, S.-B.; Duan, W.-L. *Angew. Chem., Int. Ed.* **2015**, *54*, 6265.

(11) Fernández, I.; Oña-Burgos, P.; Ruiz-Gómez, G.; Bled, C.; García-Granda, S.; López-Ortiz, F. *Synlett* **2007**, 611.

(12) (a) Steiner, A.; Zacchini, S.; Richards, P. I. *Coord. Chem. Rev.* **2002**, *227*, 193. (b) Collins, S. *Coord. Chem. Rev.* **2011**, *255*, 118.

(13) Recent references: (a) Hawley, A. L.; Stasch, A. *Eur. J. Inorg. Chem.* **2015**, *2015*, 258. (b) Prashanth, B.; Singh, S. *J. Chem. Sci.* **2015**, *127*, 315. (c) Liu, B.; Sun, G.; Li, S.; Liu, D.; Cui, D. *Organometallics* **2015**, *34*, 4063. (d) Liu, B.; Liu, D.-T.; Li, S.-H.; Sun, G.-P.; Cui, D.-M. *Chin. J. Polym. Sci.* **2016**, *34*, 104. (e) Rufanov, K. A.; Pruss, N. K.; Sundermeyer, J. *Dalton Trans.* **2016**, *45*, 1525. (f) Prashanth, B.; Singh, S. *Dalton Trans.* **2016**, *45*, 6079.

(14) Casimiro, M.; García-López, J.; Iglesias, M. J.; López-Ortiz, F. *Dalton Trans.* **2014**, *43*, 14291.

(15) Similar structural features have been found in the analogous C_{α} -lithiated *N*-methoxycarbonylphosphazene: Fernández, I.; Álvarez-Gutiérrez, J. M.; Kocher, N.; Leusser, D.; Stalke, D.; González, J.; López-Ortiz, F. *J. Am. Chem. Soc.* **2002**, *124*, 15184.

(16) (a) Beak, P.; Meyers, A. I. *Acc. Chem. Res.* **1986**, *19*, 356. (b) Beak, P.; Basu, A.; Gallagher, D. J.; Park, Y. S.; Thayumanavan, S. *Acc. Chem. Res.* **1996**, *29*, 552. (c) Basu, A.; Thayumanavan, S. *Angew. Chem., Int. Ed.* **2002**, *41*, 716. (d) Whisler, M. C.; MacNeil, S.; Snieckus, V.; Beak, P. *Angew. Chem., Int. Ed.* **2004**, *43*, 2206. (e) Tilly, D.; Magolan, J.; Mortier, J. *Chem. - Eur. J.* **2012**, *18*, 3804.

(17) (a) Bacon, J.; Gillespie, R. J.; Quail, J. W. *Can. J. Chem.* **1963**, *41*, 3063. (b) Murali, N.; Nageswara-Rao, B. D. *J. Magn. Reson., Ser. A* **1996**, *118*, 202. (c) Kofod, P. *J. Magn. Reson., Ser. A* **1996**, *119*, 219. (d) Fraenkel, G.; Subramanian, S.; Chow, A. *J. Am. Chem. Soc.* **1995**, *117*, 6300.

(18) (a) Reich, H. J.; Borst, J. P.; Dykstra, R. R. *Tetrahedron* **1994**, *50*, 5869. (b) Reich, H. J.; Holladay, J. E.; Mason, J. D.; Sikorski, W. H. *J. Am. Chem. Soc.* **1995**, *117*, 12137. (c) Reich, H. J.; Holladay, J. E.; Walker, T. G.; Thompson, J. L. *J. Am. Chem. Soc.* **1999**, *121*, 9769.

(19) (a) Reich, H. J.; Borst, J. P.; Dykstra, R. R.; Green, D. P. *J. Am. Chem. Soc.* **1993**, *115*, 8728. (b) Reich, H. J. *J. Org. Chem.* **2012**, *77*, 5471. (c) Reich, H. J. *Chem. Rev.* **2013**, *113*, 7130.

(20) Average chemical shifts calculated with respect to the corresponding signals of the diastereotopic *P*-phenyl rings of 8.

(21) Carbons were assigned on the basis of the correlations observed in the 2D $^1\text{H},^{13}\text{C}$ HMQC spectrum measured in THF- d_8 at $-100\text{ }^{\circ}\text{C}$ (Figure S7 in the Supporting Information) and the chemical shifts and magnitude of $^{31}\text{P},^{13}\text{C}$ coupling constants of the quaternary carbons.

(22) Fernández, I.; Oña-Burgos, P.; Oliva, J. M.; López-Ortiz, F. *J. Am. Chem. Soc.* **2010**, *132*, 5193.

- (23) García-López, J.; Peralta-Pérez, E.; Forcén-Acebal, A.; García-Granda, S.; López-Ortiz, F. *Chem. Commun.* **2003**, 856.
- (24) (a) Korth, K.; Sundermeyer, J. *Tetrahedron Lett.* **2000**, *41*, 5461. (b) Jantzi, K. L.; Guzei, I. A.; Reich, H. J. *Organometallics* **2006**, *25*, 5390.
- (25) (a) Seebach, D.; Hässig, R.; Gabriel, J. *Helv. Chim. Acta* **1983**, *66*, 308. (b) Wehmschulte, R. J.; Power, P. P. *J. Am. Chem. Soc.* **1997**, *119*, 2847. (c) Reich, H. J.; Green, D. P.; Medina, M. A.; Goldenberg, W. S.; Gudmundsson, B. Ö.; Dykstra, R. R.; Phillips, N. H. *J. Am. Chem. Soc.* **1998**, *120*, 7201.
- (26) (a) Bauer, W.; Schleyer, P. v. R. *Adv. Carbanion Chem.* **1992**, *1*, 89. (b) Wheatley, A. E. H. *Eur. J. Inorg. Chem.* **2003**, 2003, 3291. (c) Zabicky, J. In *The Chemistry of Organolithium Compounds*; Rappoport, Z., Marek, I., Eds.; John Wiley & Sons: New York, 2004; Chapter 8, p 311.
- (27) Carriedo, G.; García-Alonso, F. J.; García, J. L.; Carbajo, R. J.; López-Ortiz, F. *Eur. J. Inorg. Chem.* **1999**, 1999, 1015 and references therein.
- (28) Fernández, I.; López-Ortiz, F. *Chem. Commun.* **2004**, 1142.
- (29) (a) Jones, A. C.; Sanders, A. W.; Bevan, M. J.; Reich, H. J. *J. Am. Chem. Soc.* **2007**, *129*, 3492. (b) Gessner, V. H.; Däschlein, C.; Strohmann, C. *Chem. - Eur. J.* **2009**, *15*, 3320. (c) Plessel, K. N.; Jones, A. C.; Wherritt, D. J.; Maksymowicz, R. M.; Poweleit, E. T.; Reich, H. *J. Org. Lett.* **2015**, *17*, 2310.
- (30) Brunner, H.; Tsuno, T.; Balazs, G.; Bodensteiner, M. *J. Org. Chem.* **2014**, *79*, 11454.
- (31) (a) Suezawa, H.; Ishihara, S.; Umezawa, Y.; Tsuboyama, S.; Nishio, M. *Eur. J. Org. Chem.* **2004**, 4816. (b) Takahashi, O.; Kohno, Y.; Nishio, M. *Chem. Rev.* **2010**, *110*, 6049. (c) Salonen, L. M.; Ellermann, M.; Diederich, F. *Angew. Chem., Int. Ed.* **2011**, *50*, 4808.
- (32) Computations at the M06-2X(SMD,THF)/6-311+G(d,p)//B3LYP/6-31G(d) level afforded a notably larger energy difference, $\Delta G^{183}(\mathbf{8a}-\mathbf{8b}) = 2.7$ kcal/mol; see ref 14.
- (33) (a) Stuckwisch, C. G. *J. Org. Chem.* **1976**, *41*, 1173. (b) Baier, F.; Fei, Z.; Gornitzka, H.; Murso, A.; Neufeld, S.; Pfeiffer, M.; Rüdemaier, I.; Steiner, A.; Stey, T.; Stalke, D. *J. Organomet. Chem.* **2002**, *661*, 111. (c) Boubekour, L.; Ricard, L.; Mézailles, N.; Demange, M.; Auffrant, A.; Le Floch, P. *Organometallics* **2006**, *25*, 3091.
- (34) Bauer, W.; Winchester, W. R.; Schleyer, P. R. *Organometallics* **1987**, *6*, 2371.
- (35) Pratt, L. M.; Truhlar, D. G.; Cramer, C. J.; Kass, S. R.; Thompson, J. D.; Xidos, J. D. *J. Org. Chem.* **2007**, *72*, 2962.
- (36) The analogous displacement of a THF molecule from the lithium of the ^tBuLi moiety of species **11C** would afford complex **12C**, which is only slightly stabilized with respect to **8a** ($\Delta G^{183} = -1.3$ kcal/mol, Figure S12 in the Supporting Information).
- (37) The transition states **TS1C** and **TS1D** generated in the ortho deprotonation of conformers **8c** and **8d**, respectively, are additionally destabilized with respect to **TS1A**, $\Delta\Delta G^{\ddagger 183} = 2.4$ kcal/mol; see Figure S15 in the Supporting Information.
- (38) (a) Nishio, N.; Hirota, M.; Umezawa, Y. *The CH/π Interaction: Evidence, Nature and Consequences*; Wiley-VCH: New York, 1998. (b) Ganguly, H. K.; Majumder, B.; Chattopadhyay, S.; Chakrabarti, P.; Basu, G. *J. Am. Chem. Soc.* **2012**, *134*, 4661–4669. (c) Kumar, M.; Balaji, P. V. *J. Mol. Model.* **2014**, *20*, 2136.
- (39) Zhao, Y.; Truhlar, D. G. *Theor. Chem. Acc.* **2008**, *120*, 215.
- (40) Marenich, A. V.; Cramer, C. J.; Truhlar, D. G. *J. Phys. Chem. B* **2009**, *113*, 6378.
- (41) Ribeiro, R. F.; Marenich, A. V.; Cramer, C. J.; Truhlar, D. G. *J. Phys. Chem. B* **2011**, *115*, 14556.
- (42) Frisch, M. J., et al. *Gaussian 09, Revision B.01*; Gaussian, Inc., Wallingford, CT, 2010.